Bioorganic & Medicinal Chemistry 21 (2013) 1911–1917

Contents lists available at SciVerse ScienceDirect

Bioorganic & Medicinal Chemistry

journal homepage: www.elsevier.com/locate/bmc

Five-membered iminocyclitol α-glucosidase inhibitors: Synthetic, biological screening and in silico studies

Luis R. Guerreiro [a], Elisabete P. Carreiro [a], Luis Fernandes [a], Teresa A. F. Cardote [b], Rui Moreira [b], Ana T. Caldeira [a], Rita C. Guedes [b], A. J. Burke [a,*]

[a] Departamento de Química and Centro de Química de Évora, Universidade de Évora, Rua Romão Ramalho, 59, 7000 Évora, Portugal
[b] Research Institute for Medicines and Pharmaceutical Sciences-iMed.UL, Faculty of Pharmacy, University of Lisbon, Av. Prof. Gama Pinto, 1649-003 Lisbon, Portugal

ARTICLE INFO

Article history:
Received 16 November 2012
Revised 10 January 2013
Accepted 14 January 2013
Available online 26 January 2013

Keywords:
Iminocyclitol
Small molecule inhibitor
α-Glucosidase
Enantiopure compound
(3,4)-Dihydroxypyrrolidine

ABSTRACT

The design and synthesis of a small library of pyrrolidine iminocyclitol inhibitors with a structural similarity to 1,4-dideoxy-1,4-imino-D-arabitol (DAB-1) is reported. This library was specifically designed to gain a better insight into the mechanism of inhibition of glycosidases by polyhydroxylated pyrrolidines or iminocyclitols. Pyrrolidine-3,4-diol **15a** and pyrrolidine-3,4-diol diacetate **15b** had emerged as the most potent α-glucosidase inhibitors in the series. Docking studies performed with an homology model of α-glucosidase disclosed binding poses for compounds **15a**, **15b**, **16a**, and **16a′** occupying the same region as the NH group of the terminal ring of acarbose and suggest a closer and stronger binding of compound **15a** and **15b** with the enzyme active site residues. Our studies indicate that 2 or 5-hydroxyl substituents appear to be vital for high inhibitory activity.

1. Introduction

The iminocyclitols—polyhydroxylated pyrrolidines and piperidines—are a family of important pharmacologically active compounds that are both potent glycosidase and glycosyltransferase inhibitors due to their mimicry of the transition state of the enzymatic reaction, including serendipitous electrostatic binding interactions.[1,2] For this reason, they have been selected as therapeutic agents in several areas such as cancer, viral infections (particularly influenza) and diabetes, etc. For example, deoxinojirimicin (DNJ) **1** is an inhibitor of endoplasmic reticulum α-glucosidases I,[3] and 1,4-dideoxy-1,4-imino-D-arabinitol (DAB-1) **2** and 2,5-dideoxy-2,5-imino-D-mannitol (DMDP) **3**[5] are powerful inhibitors of α-glucosidases[4] (Fig. 1). The synthesis of more potent novel analogues of these compounds is an important goal in medicinal chemistry, not only for targeting human disease, but also as tools to probe the mechanism of glucosidase function. In most cases, these molecules function as pure enantiomers.

It has been previously pointed out that structure–activity relationships for iminocyclitol glycosidase inhibitors are difficult to elucidate, making rational inhibitor design a difficult task.[1] It is also known that five-membered iminocyclitols can give rise to higher inhibition than their six-membered counterparts and subtle selectivities may be observed for five- over six-membered systems, thus making logical design based upon structural analogy difficult.[6] For this reason many types of five-membered iminocyclitols have been synthesized and screened. An examination of the literature showed that a number of diverse structural types have been screened for α-glucosidase inhibition. This includes those developed by Davis, for example, **4**[6] (Fig. 1) obtained from 3-pyrroline and tartaric acid, and showed no significant inhibition (3–13% at the 1 mM level). The five-membered iminocyclitol amide derivatives **5** developed by Wong's group showed inhibition with a K_i value of 53 nM[7] (which was better than that exhibited by the parent structure **6**) and the 2-alkylated analogues of type **7** (Fig. 1) were also shown by Wong[1b] to be weak α-glucosidase inhibitors (3–54% inhibition at 200 μM). Davis has also shown that a library of *N*-acyl(aroyl)-2-carboxyamide substituted pyrrolidine iminocyclitols of type **8**, showed little or no inhibition at 100 μM.[8] Wong has prepared and tested pyrrolidine iminocyclitols of type **9** with side-chains in both the 2 and the 5 positions,[9] in which some were very potent inhibitors. Calveras et al.[10] showed that a library of iminocyclitols of type **10** inhibited this enzyme at 1.6–4.2 nM level. In most cases the presence of a hydroxymethyl appendage seems to give significant inhibition, whereas when substituted by an alkyl group, as in **4** and **7** (Fig. 1), the inhibition is weaker or even absent, indicating that this substituent must be relevant to approximate the structures of the natural α-glucosidase sugar substrate.[6] This point has been echoed by Wong[9] and indeed, this hypothesis has been supported somewhat by the work of both Bols[11] and Lundt,[12] who prepared the 2,5-non-substituted pyrrolidine iminocyclitols **11**, **12** and **13**, with the hydroxymethyl appendage transposed to

* Corresponding author. Tel.: +351 266745310

0968-0896/$ - see front matter © 2013 Elsevier Ltd. All rights reserved.
http://dx.doi.org/10.1016/j.bmc.2013.01.030

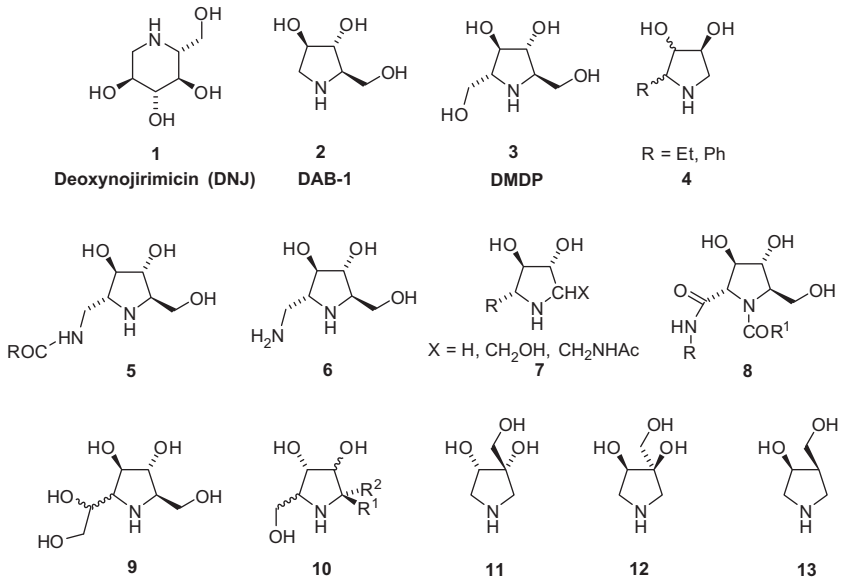

Figure 1. Some natural and iminocyclitol inhibitors.

the 3-position and showing weak and unspecific inhibition (at 3.8 mM for **11** and 2 mM in the case of **12**)[11] and a α-glucosidase inhibition in the case of **13** (at 0.8 mM).[12] It must be noted that the 3,4-hydroxy groups in these iminocyclitols had a *cis* relative configuration. However, on the other hand, in the case of the study conducted by Calveras et al.[10] the results seemed to imply that the hydroxymethyl group could have a deleterious effect on the activity of the enzyme.

We were curious to know how important these structural/functional appendages were for α-glucosidase inhibition and thus set about preparing a very small library of simple pyrrolidine iminocyclitols lacking functionality in the 2-position and with or without a hydrophobic group on the pyrrolidine nitrogen. The diol unit had the *trans*-configuration. Asano's group also studied this question several years ago, and speculated that glycoside inhibitors have structures which resemble those of the respective cations.[13] In fact, the binding mode of the five-membered inhibitors has yet eluded characterization. Work with the endoglycoceramidase model systems by Withers' group[2] using a variety of five- and six-membered iminocyclitol inhibitors has shown that imitation of the substrate's 2-hydroxy group by the inhibitor's 6-hydroxy group and by electrostatic interactions between the ring nitrogen and the glutamic acid residues (which are also present in α-glucosidases[14]) are important.

For testing purposes, Davis and co-workers synthesized a small library of anisomycin analogues **14** (Fig. 2). These were designed on the basis that a hydrophobic group at/or near the putative aglycone binding site might augment enzyme inhibition.[6] In fact, the application of anisomycin and analogues as inhibitors against glycosidases has been very poorly studied. These compounds indeed displayed competitive inhibition of α-glucosidases.[6]

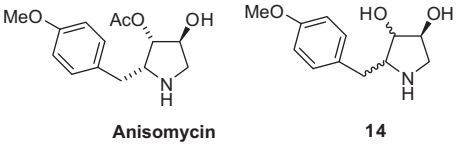

Figure 2. Anisomycin and anisomycin analogues tested by Davis.[6]

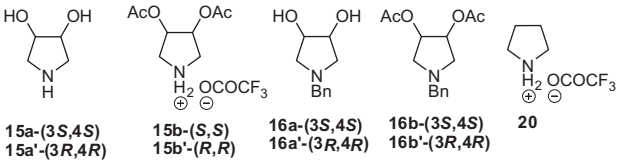

Figure 3. Library of five-membered iminocyclitols derived from L- or D-tartaric acid.

In order to probe the inhibition mechanism of such inhibitors on α-glucosidases, we decided to use a small library of enantiomerically pure five-membered iminocyclitol inhibitors of the enantiomeric series derived from L- and D-tartaric acids (Fig. 3, all with the *trans*-relative stereochemistry), lacking substituents in either the 2 or 5-positions and some containing acetate groups to increase the hydrophobicity of the inhibitor and to protect the hydroxyl groups. Molecular modeling studies involving a docking protocol were undertaken on a completely new and validated homology model of α-glucosidase with the purpose to clarify these compounds inhibitory potency with yeast maltase. An additional goal was to test some simple, easily prepared pyrrolidine diols aswell.

2. Results and discussion

2.1. Chemistry

The (3*R*,4*R*)-pyrrolidine-3,4-diol **15a** (Scheme 1) was synthetized using the method of Nagel.[16] This molecule has previously been used as an intermediate in the synthesis of certain asparagine modified pyrrolidine iminocyclitols used as Multiple Sclerosis Antigenic probes.[15] Incidentally **16a** has been synthesized previously in our group, by an innovative, but less direct route which uses the commercial dioxane diester **17** (Scheme 1) derived from the tartaric acid as precursor.[17] **16b** was obtained in a yield of 92% from **16a** by stirring in the presence of pyridine and acetic anhydride (Scheme 1). The diacetate derivative **15b** (as the trifluoroacetate salt) was obtained despite many efforts according to the procedure shown in Scheme 2. Many unsuccessful debenzylations were carried out, via hydrogenation of the *N*-benzyl diacetate derivative **16b** with palladium on carbon, or with iron chloride.[18]

An alternative, more indirect synthetic route was used that involved the transformation of both enantiomers **15a** and **15a′** to the *N*-Boc protected intermediates (structures not shown) followed by successful acetylation to the *N*-Boc protected diacetates **19a**, and **19a′** (Scheme 2). The deprotection of **19a** was investigated using several methods, but it was successfully transformed to the corresponding (3*S*,4*S*)-3,4-diacetoxypyrrolidinium trifluoroacetate **15b** in 98% yield using TFA in dichloromethane. The other methods which failed to function, included, (a) HCl 4 M in THF,[19] (b) TBAF in THF,[20] (c) Na_2CO_3/DME/H_2O[21] and (d) Amberlyst 15/NH_4OH.[22] In the case of (a), both deprotection of the *N*-Boc and acetyl groups occurred to give **15a**. In the case of (b) and (c) the acetyl groups were removed. In the case of (d), compound **15a** was obtained due to hydrolysis of the acetyl groups by the aqueous basic conditions employed. Compound **20** was synthetized using 1 equiv of TFA and pyrrolidine in dichloromethane. This compound was used as a reference in the enzymatic bioassays.

The same procedures were used to obtain compounds **15b′**, **16a′** and **16b′** (the enantiomeric series) derived from D-tartaric acid. The NMR and other physical data for these compounds were in agreement with that obtained from the literature.[15]

2.2. Biological screening studies

These compounds were then assayed for the inhibition of the α-glucosidase from *Saccharomyces cerevisiae* using inhibitor concentrations of between 0.19×10^{-3} and 46 mM. This α-glucosidase contains 584 amino acid residues (vide infra). In our bioassays, eight compounds (**15a**, **15b**, **15b′**, **16a**, **16a′**, **16b**, **16b′** and **20**) were tested, but only four (**15a**, **15b**, **16a**, **16a′**) showed an inhibition profile in the concentration range used, exhibiting over 50% inhibition down to a concentration of $\geqslant$10.9 mM (Fig. 4). The debenzylated compounds **15a** and **15b** were the best inhibitors, with IC_{50}'s of 10.9 and 12.5 mM, respectively (Table 1). In the case of compounds **15b** and **15b′**, which are enantiomers, only **15b** showed an inhibition profile in the concentration range used, exhibiting >50% inhibition at a concentration of 25 mM (80% of inhibition) and at this concentration **15b′** showed only 40% inhibition. By using **20** as a control, it was established that the $^{-}OCOCF_3$ counter-ion had no effect on the α-glucosidase activity, no inhibitory activity was observed at over 50% of the inhibition concentration. Compounds **16a** and **16a′**, inhibited the enzyme over the 50% of the inhibition concentration, and had IC_{50}'s of 38 and 25 mM, respectively (Table 1). Compound **16a′** had the best inhibition profile. In the case of **16b** and **16b′** no inhibitory activity was observed at the concentrations studied.

In summary, compound **15a** showed the greatest inhibitory activity, whilst **16a** was the least active. We also screened the pseudotetrasaccharide α-glucosidase inhibitor, acarbose, which is a known competitive inhibitor, and used as a cheap benchmark for the level of inhibition exhibited by our iminocyclitols. An IC_{50} value of 0.641 mM was observed for acarbose, much higher than that of our best inhibitor **15a**. Acarbose was shown to be active against this enzyme by Ferreira and co-workers,[23] showing an IC_{50} value of 0.109 mM, but this was obtained under different experimental conditions. Comparing the compounds **16a** and **16a′** with **16b** and **16b′** it would appear that the presence of free hydroxyl groups in the 3 and 4-positions is important in the inhibition process, possibly due to favorable secondary hydrogen-bonding interactions.

Given that the inhibition values for the unsubstituted pyrrolidines were only 2–3 times stronger than for the benzylated analogues (Table 1), it is hard at this juncture to clearly conclude that the presence of a free amine group is necessary for good inhibition of this enzyme. The difference in inhibitory activities between the *o*-acetylated and non-acetylated derivatives (compare **15a** with **15b** in Table 1) was virtually nil, this close similarity we believe might have been a consequence of the hydrolysis of the acetate groups during the assays. Based on these observations, and from the analogous work of Withers and Davis[24,25] on the inhibition of the glucosidase hydrolase endocellulase Cel5A from *Bacillus agaradhaerens* using isofagomine as the probe, and in the knowledge that the catalytic residues of the active site of the α-glucosidase from *S. cerevisiae* consists of three amino acids, two aspartic acids (Asp214 and Asp349) and one glutamic acid (Glu276) which acts as a proton donor,[23] including key Tyr71, His111 and His348 units in the substrate binding domain of the enzyme,[23] we present the following putative preliminary model (Fig. 5), which on the basis of the weakly acidic conditions of the assay (pH 6.7) and literature precedent should be protonated on the pyrrolidine nitrogen.

Continuing with the same argument as given above, observing that the difference in the inhibitory activities for both **16a** and **16a′** was less than twofold, it is hard to draw any strong conclusions as to the stereochemical requirements for inhibition.

In order to gain a better insight into the process of inhibition at the molecular level we conducted some molecular modeling studies or more precisely, docking studies.

2.3. Molecular modeling studies

In order to rationalize the described biological results, docking studies of compounds **15a**, **15b**, **16a**-(3*S*,4*S*), and **16a′**-(3*R*,4*R*) and **16b** were undertaken. Molecular docking simulations were performed, using GOLD software version 5.1.0,[26] to predict the interactions and binding modes of the synthesized compounds on the α-glucosidase active site and to evaluate their relative binding affinities. To better understand the important enzyme–ligand interactions, poses inside the binding pocket were performed. As a means of testing the adopted scoring function, some known inhibitors like acarbose (the first α-glucosidase inhibitor approved for type 2 diabetes treatment), DAB-1, and DMDP were also docked within the MAL12 model active site.

Although the X-ray crystal structures of some bacterial α-glucosidases have been reported, structural information is still unavailable for the eukaryotic α-glucosidase enzyme from Baker's yeast (the enzyme used in our biological assays). However, only a few homology models have been previously developed for this enzyme. Based on the fact that the catalytic residues (Asp214, Glu276, and Asp349) and other important residues for substrate binding are highly conserved in the GH13 family, Park et al.[28] developed a MAL12 model based on oligo-1,6-glucosidase enzyme from *Bacillus cereus* (PDB code 1UOK), however this enzyme only shares a very small sequence identity (~38%). Also Ferreira and co-workers,[23] very recently developed another Mal12 homology model from *Thermotoga maritima* 4-α-glucanotransferase (PDB code 1LWJ). [29] None of these models have their 3D coordinates publicly released. Therefore we built by homology modeling a completely new α-glucosidase MAL12 model based on the crystal structure of isomaltase from *S. cerevisiae* (3AJ7.pdb)[27] recently released, isolated and in complex with its competitive inhibitor maltose. This enzyme shares 72.4% sequence identity with α-glucosidase enzyme from Baker's yeast (Fig. 2 in Supplementary data). The α-glucosidase MAL12 model developed in our study consists of a single polypeptide chain constituted of 584 residues (Fig. 6). A more complete description of the developed homology model can be found in the Experimental section.

After completing the MAL12 model, the α-glucosidase–ligand complexes were generated by docking our compounds into the enzyme active site. All the docked compounds were previously energy-minimized and subjected to 1000 docking runs (see more

details in the Experimental section). The 10 top solutions (the ones with the highest Goldscore) were visually and critically analyzed.

Interestingly, we found that all the tested compounds occupy almost the same region of the binding pocket as the amino group and its corresponding cyclohexenyl ring of acarbose. This proves that our five-membered iminocyclitol derivatives are molecules that can be favorably positioned in the binding cavity, having the capacity for forming important contacts with the enzyme active site residues.

Compound **15a**, the most potent compound in the series, forms an H-bond between the pyrrolidine nitrogen and Asp214 (1.6 Å), and also strongly interacts with Glu276 (catalytic site). The free hydroxyl groups interact with Arg439 and Asp68 and an additional interaction between the iminocyclitol and Tyr71 is also established. A very similar pose is observed for compound **15b**, however, this compound is closer to the catalytic binding site than the former due to strong interactions of the acetate groups with Arg439 and Asp68 that pushes this compound deep inside the binding site. This compound makes H-bonds with Asp214 (1.5 Å), Asp349 (1.9 Å), and Glu276 (1.6 Å).

Compound **16a** interacts with the same residues of the catalytic site, however with slightly longer interactions (~2 Å), including those in the binding region—Arg439 and Asp68. Compound **16a′**'s position is almost the same as **16a** the only difference being, the iminocyclitol ring is slightly tilted, but it establishes more interactions with the residues in the binding pocket, and thus would be expected to have a better biological activity profile than **16a**, which was observed from the biological assays. Furthermore, compound **16b**, inactive against α-glucosidases, has a completely different position inside the pocket, in this case a single interaction is established with Glu276, with one of the acetate groups pointing to the inside of the binding pocket and rotating the conformation, contrarily to the other docked compounds where the iminicyclitol ring occupies this position. This completely different pose of compound **16b** might explain the absence of activity of this compound.

The predicted poses for compounds **15a**, **15b**, **16a**, **16a′** (with inhibitory activity), and **16b** (inactive) and their interaction with the MAL12 model active site are shown in Figure 7.

As described above it can be seen that for all the bioactive compounds the iminocyclitol moiety is positioned almost at the same location, with the pyrrolidine nitrogen directed to the catalytic site (Asp214, Glu276, Asp349) and leaving the hydroxyl and acetate groups free to interact with the Asp68 and Arg439 residues. In fact, we see that the most active compounds of the series (**15a** and **15b**) are at H-bond or short distances from the catalytic residues, obviously due to the fact that these two compounds have their pyrrolidine nitrogen unsubstituted thus permitting a closer interaction with the catalytic residues. In the case of compounds **16a** and **16a′** these interactions exist, however with longer distances. What might explain the reduced inhibitory activity of these compounds? One possible explanation for the activity of these four compounds against α-glucosidases is certainly the establishment of strong (considering the short distances) interactions like, presumably, hydrogen bonds; also, the molecules seem to fit perfectly in the active site pocket. Also in agreement with bioassays our calculations suggest that compound **16b** (inactive against α-glucosidase) adopts a completely different orientation within the binding pocket when compared to the active compounds.

We consider that one limiting factor in this docking procedure was the absence of water molecules in the docking calculations. As observed in the crystallographic structure (3AJ7.PDB) this pocket accommodates several water molecules that usually help in the establishment of H-bond interactions with the free hydroxyl groups what could push the inhibitors closer to the Glu276, thus improving the interactions within the active site. This might be one reason to explain why **15a** has a slightly better activity than

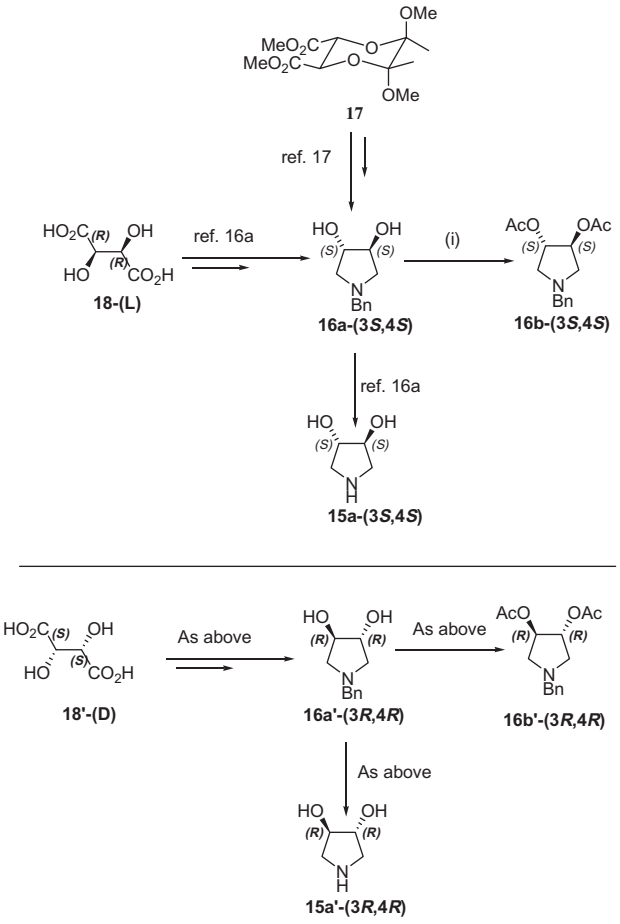

Scheme 1. Reagents and conditions: (i) Ac_2O, pyridine, rt, 8 h.

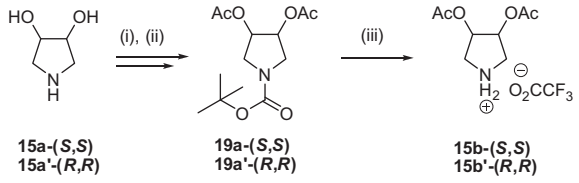

Scheme 2. Reagents and conditions: (i) BOC_2O, EtOH, 0 °C, (ii) pyridine, Ac_2O rt, 8 h, (iii) TFA, DCM, rt, 1.5 h.

15b, despite the fact that our docking studies (without water) seem to predict that the latter would be more active.

3. Experimental Section

3.1. General chemical

All reagents were obtained from Aldrich, Fluka, Alfa Aesar or Acros. Solvents were dried using common laboratory methods. (3*S*,4*S*)-Pyrrolidine-3,4-diol **15a** and (3*R*,4*R*)-Pyrrolidine-3,4-diol **15a′** were synthesized according to the method of Nagel.[16] The compounds **16a** and **16b** (and their respective enantiomers) were synthesized using the precursors (3*R*,4*R*)-*N*-benzyl-3,4-dihydroxy-2,5-dioxopyrrolidine and (3*S*,4*S*)-*N*-benzyl-3,4-dihydroxy-2,5-dioxopyrrolidine, respectively, both enantiomers had an enantiomeric purity of 99%ee as determined by HPLC. TLC was carried out on aluminium backed Kiselgel 60 F_{254} plates (Merck). Plates were visualised either by UV light or with phosphomolybdic

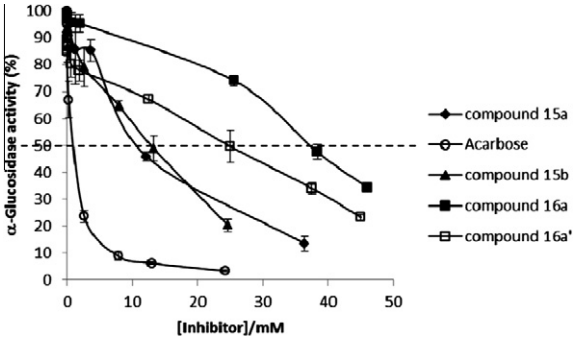

Figure 4. Inhibitory effects of compounds **15a**, **15b**, **16a, 16a**′and acarbose against α-glucosidase activity.

acid in ethanol. The ^{1}H NMR and ^{13}C NMR spectra were recorded on a Bruker Avance instrument (^{1}H: 400 MHz and ^{13}C: 100 MHz) using $CDCl_3$ as solvent and the signal from residual $CHCl_3$ as an internal standard. Mass spectra were recorded using the electrospray ionization (ESI) technique on a Bruker Daltonics Apex-Qe instrument (CACTI). Specific rotations were measured on a Perkin–Elmer 241 polarimeter.

3.2. General enzymatic assays

The assay mixture had the following composition: 50 μL of 0.1 M phosphate buffer (pH 6.7), 50 μL of 2 mM *p*-nitrophenyl-α-D-glucopyranoside (the method was optimized giving K_m and V_{max} values of 0.258 mM and 0.0418 mM min^{-1} mg^{-1}, respectively) and 50 μL of Baker's yeast α-glucosidase solution (0.04 U/mL). All the samples were run in 5 replicas. The test samples were dissolved in 2% DMSO in 0.1 M phosphate buffer (pH 6.7) and 50 μL solutions having the following range of concentration: 0.19×10^{-3} and 46 mM. The α-glucosidase activity was determined by monitoring the *p*-nitrophenol released from *p*-nitrophenyl-α-D-glycopyranoside spectrophotometrically at 405 nm over 20 min. The IC_{50} values were obtained from the inhibition curves. These determinations were made using an Elisa Microplate spectrophotometer UV/Vis (Ref. ELX800G) from Bio-Tek Instruments Inc.

3.3. Molecular modeling

3.3.1. MAL12 model building and validation

Homology modeling of α-glucosidase (MAL12) from baker's yeast was carried out to predict its 3D-structure. The amino acid sequence of α-glucosidase (MAL12) from baker's yeast comprises 584 amino acid residues and was retrieved from UniProt protein resource data bank (http://www.uniprot.org/), under the access code P53341 (http://www.uniprot.org/uniprot/P53341.html). Using the Molecular Operating Environment program (MOE) version 2011.10 (http://www.chemcomp.com/software-moe2011.htm) we searched for proper structural templates on the PDB database of protein structures and sequences and aligned the obtained results. MOE-Align implements a modified version of the alignment methodology originally introduced by Needleman and Wunsch.[30] All the default settings in the MOE-Align panel were used for the sequence alignment. Our calculations identified the *Saccharomyces cerevisiae* isomaltase crystallographic structure (PDB code 3AJ7, 1.30 Å resolution)[27] with 72.4% of sequence identity with the target as the most suitable template. Yamamoto et al.[27] resolved the structures of isomaltase of *Saccharomyces cerevisiae* (PDB code 3AJ7, 1.30 Å) and in a complex with maltose (PDB code 3A4A, 1.60 Å). The catalytic site is highly conserved in both structures (as can been seen in Fig. 1 of the Supplementary data). The 3D homology models were built with MODELLER[31] software using only a single template. A set of 10 intermediate models were generated and refined with AMBER99 (R-field) forcefield[32] and the best of them was selected and evaluated to investigate the stereochemical fitness of our model with MOE software. The stereochemical quality of the enzyme backbone and side chains was validated by Ramachandran plots. To validate our model we first docked maltose, into the structure's active site and compared the final docked complex with the crystallographic structure obtained by Yamamoto et al.[27] We confirmed that in the MAL12 model, maltose was placed in the same position as that adopted in the crystallographic structure (PDB ID: 3A4A.pdb, 1.60 Å) interacting with the active site residues in an analogous manner.

Table 1
IC_{50} values of **15a**, **15b**, **16a** and **16a**′ for α-glucosidase inhibition (*Saccharomyces cerevisiae*)

Inhibitor	IC_{50} (mM)
Acarbose	0.641
15a	10.9
15b	12.5
16a	38.0
16a′	25.0

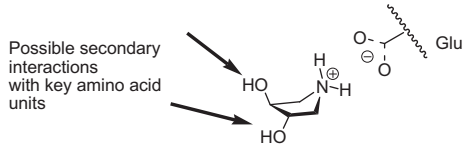

Figure 5. Schematic model to explain the possible positive secondary interactions between the α-glucosidase and inhibitor **15a**.

3.3.2. MAL12 binding site definition

MAL12 binding site is composed of Asp214, Glu276, and Asp349 catalytic residues. In addition to the catalytic residues, molecular docking studies confirm Asp68, Tyr71, and Arg439 as important residues in the α-glucosidase inhibition.

3.3.3. Docking calculations

The molecular structures of the 5-membered iminocyclitols were built and optimized with the MMFF94x forcefield as implemented in the MOE software (version 2011.10). These compounds were docked into the MAL12 model enzyme binding site. Molecular docking simulations were performed, using GOLD (Genetic Optimization Ligand Docking) software (version 5.1.0). GOLD uses an evolutionary genetic algorithm to optimize the docked conformation of the flexible inhibitor within the enzyme. For each compound, 1000 docking runs were performed. The following genetic algorithm parameters were used: population size = 100; selected pressure = 1.1; number of operations = 1000; number of islands = 5; niche size = 2; migrate = 10; mutate = 95; crossover = 95. Each conformation was ranked according to its goldscore scoring function. The top solutions (the ones with the highest goldscore[33]) were visually inspected and critically evaluated and for each inhibitor the highest scoring conformation was chosen as the actual binding conformation (Fig. 7).

3.4. Synthesis of pyrrolidine iminocyclitol inhibitors

3.4.1. (3*S*,4*S*)-*N*-Benzyl-3,4-dihydroxypyrrolidine 16a

(3*S*,4*S*)-*N*-Benzyl-3,4-dihydroxypyrrolidine **16a** was synthesized according to the method of Nagel.[16] $[\alpha]_D^{20}$ +40 (*c* 0.7 in Methanol) [$[\alpha]_D^{20}$ +32.4 (*c* 4.2 in Methanol)].[16a]

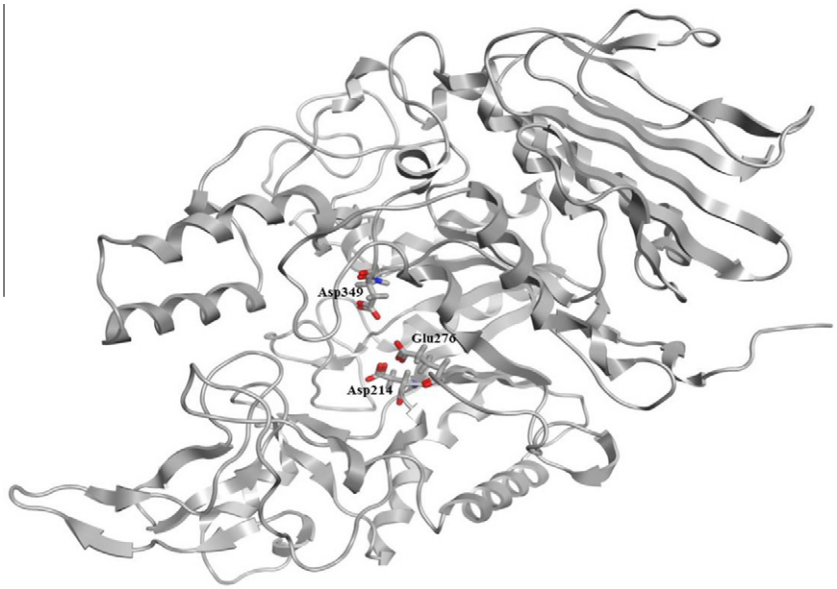

Figure 6. Graphic representation of the homology modeling structure of MAL12 with catalytic residues highlighted.

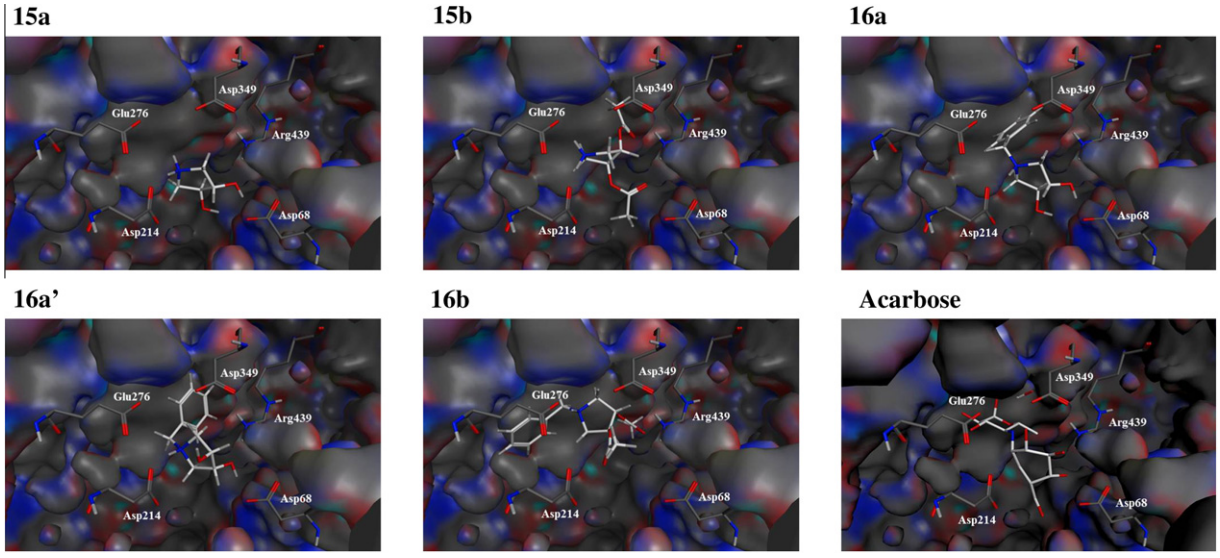

Figure 7. Binding mode of compounds **15a**, **15b**, **16a**, **16a′**, **16b** and acarbose in the MAL12 active site of the homology model.

3.4.2. (3*R*,4*R*)-*N*-Benzyl-3,4-dihydroxypyrrolidine 16a′

(3*R*,4*R*)-*N*-Benzyl-3,4-dihydroxypyrrolidine **16a′** was synthesized according to the method of Nagel.[16] $[\alpha]_D^{20}$ −28.2 (*c* 1.05 in Methanol).

3.4.3. (3*S*,4*S*)-*N*-Benzyl-3,4-pyrrolidinediol diacetate 16b

(3*S*,4*S*)-*N*-Benzyl-3,4-dihydroxypyrrolidine **16a** (2 g, 10 mmol) was dissolved in pyridine (10.5 mL) and acetic anhydride (7.7 mL). The solution was stirred for 23 h at rt. The solvents were removed in vacuo, and the mixture was dissolved in water (25 mL) and extracted with EtOAc (2 × 15 mL). The organic phases were collected, dried with $MgSO_4$, filtered and the solvent was removed, the crude product was purified by column chromatography (SiO_2, (2:1) to (1:1) Hex:EtOAc) to give the *title compound* as a light brown oil (1.12 g, 93%). ^{1}H NMR ($CDCl_3$, 400 MHz) δ: 2.05 ppm(s, 6H); 2.52 (dd, *J* 4, 12 Hz, 2H); 3.04–3.08 (m, 2H); 3.59 (d, *J* 12 Hz, 1H, *AB system*); 3.66 (d, *J* 12 Hz, 1H, *AB system*); 5.12 (s broad, 2H); 7.25–7.31 (m, 5H). ^{13}C NMR ($CDCl_3$, 100.61 MHz) δ: 170.4 ppm, 137.5, 128.9, 128.4, 127.3, 77.7, 59.7, 58.1, 21.0. MS (ESI-TOF), 278.14 (M+1).

3.4.4. (3*R*,4*R*)-*N*-Benzyl-3,4-pyrrolidinediol diacetate 16b′

Using the same procedure as described previously with **16a′** as the substrate, and in the same quantities, the *title compound* was obtained as a light brown oil (0.96 g, 81.5%). The NMR data were similar to **16b**.

3.4.5. (3*R*,4*R*)-1-(*tert*-Butoxycarbonyl)-3,4-pyrrolidinediol diacetate 19a′

(3*R*,4*R*)-Pirrolidine-3,4-diol **15a′** (0.848 g, 8.23 mmol) was dissolved in ethanol (35 mL) this was followed by the slow addition of Boc-anhydride at 0 °C. The mixture was stirred for 23 h at 0 °C. The reaction was warmed to 50 °C and stirred for over 1 h, and the solvents were removed in vacuum to give a brown solid. To the crude product was added pyridine (4.5 mL) and Ac_2O (5.6 mL) and stirred for 19 h at rt. The solvent was removed in

vacuum and the crude product was purified by column chromatography [SiO_2, (2:1) to (1:1) Hex:EtOAc] to give the *title compound* **19a′** as a colorless oil (1.8 g, 76%) ^{1}H NMR (400 MHz, $CDCl_3$): δ = 1.43 ppm (s, 9H), 2.04 (s, 6H), 3.38 (d, *J* 12 Hz, 1H), 3.48 (d, *J* 12 Hz, 2H), 3.66–3.63 (m, 2H), 5.09 (s broad, 2H). ^{13}C NMR (100 MHz, $CDCl_3$): δ = 20.8 ppm, 28.3, 49.6, 50.1, 74.2, 75.1, 79.9, 154.2, 169.6, 169.7. MS (ESI-TOF), 288.15 (M+1).

3.4.6. (3*S*,4*S*)-1-(*tert*-Butoxycarbonyl)-3,4-pyrrolidinediol diacetate 19a

Using the same procedure as described previously: **15a** (0.750 g, 7.27 mmol), Boc-anhydride (1.22 g, 10.2 mmol) in ethanol (20 mL) as solvent. Acetylation was conducted with pyridine (5.6 mL) and acetic anhydride (4.5 mL) to give the *title compound* **19a** as a colorless oil (0.868 g, 42%). The NMR data was similar to **19a′**. $[\alpha]_D^{20}$ +30 (*c* 1.08 in $CHCl_3$).

3.4.7. (3*R*,4*R*)-3,4-Diacetoxypyrrolidinium 2,2,2-trifluoroacetate 15b′

(3*R*,4*R*)-1-(*tert*-Butoxycarbonyl)-3,4-pyrrolidinediol diacetate **19a′** (0.4 g, 1.39 mmol) was dissolved in dichloromethane (4 mL) this was followed by the addition of TFA (4 mL) and the mixture was stirred at rt for 1.5 h (TLC analysis revealed the presence of no substrate). The mixture was evaporated in vacuo to give a brown oil (0.255 g, 98%). ^{1}H NMR (400 MHz, $CDCl_3$) δ: 2.09 ppm (s, 6H), 3.51 (d, *J* 12 Hz, 2H), 3.65 (dd, *J* 4, 12 Hz, 2H), 5.25 (d, *J* 4 Hz, 2H), 10.23 (s broad, 2H). ^{13}C NMR (100 MHz, $CDCl_3$): δ = 20.4 ppm, 49.0, 74.2, 169.5. MS (ESI-TOF), 188.1 (M).

3.4.8. (3*S*,4*S*)-3,4-Diacetoxypyrrolidinium 2,2,2-trifluoroacetate 15b

Using the same procedure as described previously: **19a** (0.300 g, 1.04 mmol), CH_2Cl_2 (2 mL) and TFA (2 mL) the *title compound* **15b** was obtained as a brown oil (0.190 g, 98%). The NMR data was similar to **15b′**.

4. Conclusions

We have successfully synthesized a small library of *trans*-pyrrolidine α-glucosidase inhibitors, lacking functionality in either the 2 or 5 positions. These compounds were assayed for baker's yeast α-glucosidadse inhibition using acarbose as a reference. It was the non-benzylated diol **15a** which showed the highest inhibition (IC_{50} = 10.9 mM). It seems that the presence of a free NH group and free hydroxyl groups in the 3 and 4 positions are important for favorable interaction with the enzyme active site. However, this study reinforces the fact that in order to have micromolar levels of inhibition or better (like in the examples shown above) it is necessary to have substituents in the 2 and/or 5 positions.

A molecular modeling study using a completely new MAL12 enzyme homology model was carried out and explains the inhibitory activity of the tested compounds. Our docking studies explain the improved inhibitory activity of **15a** and **15b** based on the distances and interactions that these compounds establish with the active site catalytic residues. We are currently investigating these molecules and other analogues for the inhibition of mammalian α-glucosidases, and other carbohydrate-processing enzymes. We are also looking at saturation transference difference-NMR (STD-NMR) as another method to probe these very interesting interactions.

Acknowledgements

EPC thanks the Fundação para a Ciência e a Tecnologia (FCT) for a post-doctoral research fellowship (SFRH/BPD/72182/2010). The personnel of the mass spectrometry unit at C.A.C.T.I (Univ. of Vigo, Spain) are acknowledged for mass spectrometric analyses. Dr. Olivia Furtado of the Laboratorio Nacional de Energia e Geologia (LNEG), is acknowledged for the optical rotation measurements. We also thank Miss Mariana Moreira, for her assistance in the exploratory deprotection studies leading to **15b** and its enantiomer.

Supplementary data

Supplementary data associated with this article can be found, in the online version, at http://dx.doi.org/10.1016/j.bmc.2013.01.030.

References and notes

1. For key references. (a) Lillelund, V. H.; Jensen, H. H.; Liang, X.; Bols, M. *Chem. Rev.* **2002**, *102*, 515; (b) Sugiyama, M.; Hong, Z.; Liang, P.-H.; Dean, S. M.; Whalen, L. J.; Greenberg, W. A.; Wong, C.-H. *J. Am. Chem.* **2007**, *129*, 14813. , and references cited therein; For more specific references see: Moorthy, N. S. H. N.; Bras, N. F.; Ramos, M. J. *Bioorg. Med. Chem.* **2012**, *20*, 6945; Bello, C.; Cea, M.; Dal Bello, G.; Garuti, A.; Rocco, I.; Cirmena, G.; Moran, E.; Nahimana, A.; Duchosal, M. A.; Fruscione, F.; Pronzato, P.; Grossi, F.; Patrone, F.; Ballestrero, A.; Dupuis, M.; Sordat, B.; Nencioni, A.; Vogel, P. *Bioorg. Med. Chem.* **2010**, *18*, 3320; Moreno-Clavijo, E.; Carmona, A. T.; Vera-Ayoso, Y.; Moreno-Vargas, A. J.; Bello, C.; Vogel, P.; Robina, I. *Org. Biomol. Chem.* **2009**, *7*, 1192.
2. Caines, M. E. C.; Hancock, S. M.; Tarling, C. A.; Wrodnigg, T. M.; Stick, R. V.; Stütz, A. E.; Vasella, A.; Withers, S. G.; Strynadka, N. C. J. *Angew. Chem.* **2007**, *46*, 4474.
3. Inouye, S.; Tsurouka, T.; Ito, T.; Niida, T. *Tetrahedron* **1968**, *24*, 2125.
4. Kim, Y. J.; Kido, M.; Bando, M.; Kitahara, T. *Tetrahedron* **1997**, *53*, 7501.
5. Schofield, A. M.; Fellows, L. E.; Nash, R. J.; Fleet, G. W. J. *Life Sci.* **1986**, *39*, 645.
6. Chapman, T. M.; Courtney, S.; Hay, P.; Davis, B. G. *Chem. Eur. J.* **2003**, *9*, 3397. and references cited therein.
7. Liang, P.-H.; Cheng, W.-C.; Lee, Y.-L.; Yu, H.-P.; Wu, Y.-T.; Lin, Y.-L.; Wong, C.-H. *ChemBioChem* **2006**, *7*, 165.
8. Chapman, T. M.; Davies, I. G.; Gu, B.; Block, T. M.; Scopes, D. I. C.; Hay, P. A.; Courtney, S. M.; McNeill, L. A.; Schofield, C. J.; Davis, B. G. *J. Am. Chem. Soc.* **2005**, *127*, 506.
9. Takebayashi, M.; Hiranuma, S.; Kanie, Y.; Kajimoto, T.; Kanie, O.; Wong, C.-H. *J. Org. Chem.* **1999**, *64*, 5280.
10. Calveras, J.; Egido-Gabás, M.; Gómez, L.; Casas, J.; Parella, T.; Joglar, J.; Bujons, J.; Clapés, P. *Chem. Eur. J.* **2009**, *15*, 7310.
11. Bols, M. *Tetrahedon Lett.* **1996**, *37*, 2097.
12. Godskesen, M.; Lundt, I. *Tetrahedon Lett.* **1998**, *39*, 5841.
13. Asano, N.; Oseki, K.; Kizu, H.; Matsui, K. *J. Med. Chem.* **1984**, *37*, 3701.
14. Protein Data Bank. http://www.rcsb.org.
15. Nuti, F.; Paolini, I.; Cardona, F.; Chelli, M.; Lolli, F.; Brandi, A.; Goti, A.; Rovero, P.; Papini, A. M. *Bioorg. Med. Chem.* **2007**, *15*, 3965.
16. (a) Nagel, U.; Kinzel, E.; Andrade, J.; Prescher, G. *Chem. Ber.* **1986**, *119*, 3326; (b) Beck, W.; Nagel, U. U.S. patent 4634,775, 1985.
17. Martins, J. G.; Barrulas, P. C.; Marques, C. S.; Burke, A. J. *Synth. Commun.* **2008**, *38*, 1365.
18. Guerreiro, L. R.; Simões, M.; Carreiro, E. P.; Burke, A. J. *unpublished results*.
19. Greene, T. W.; Wuts, P. G. M. *Protective Groups in Organic Synthesis*, 3rd ed.; John Wiley & Sons, Inc: New York, 1999.
20. Kazzouli, S. E.; Koubachi, J.; Berteina-Raboin, S.; Mouaddib, A.; Guillaumet, G. *Tetrahedron Lett.* **2006**, *47*, 8575.
21. Routier, S.; Saugé, L.; Ayerbe, N.; Coudert, G.; Mérour, J.-Y. *Tetrahedron Lett.* **2002**, *43*, 589.
22. Liu, Y.-S.; Zhao, C.; Bergbreiter, D. E.; Romo, D. *J. Org. Chem.* **1998**, *63*, 3471.
23. Ferreira, S. B.; Sodero, A. C. R.; Cardoso, M. F. C.; Lima, E. S.; Kaiser, C. R.; Silva, F. P.; Ferreira, V. F. *J. Med. Chem.* **2010**, *53*, 2364.
24. Varrot, A.; Tarling, C. A.; Macdonald, J. M.; Stick, R. V.; Zechel, D. L.; Withers, S. G.; Davies, G. J. *J. Am. Chem.* **2003**, *125*, 7496.
25. Zechel, D. L.; Withers, S. G. *Acc. Chem. Res.* **2000**, *33*, 11.
26. Jones, G.; Willett, P.; Glen, R. C. *J. Mol. Biol.* **1995**, *245*, 43; Jones, G.; Willett, P.; Glen, R. C.; Leach, A. R.; Taylor, R. *J. Mol. Biol.* **1997**, *267*, 727.
27. Yamamoto, K.; Miyake, H.; Kusunoki, M.; Osaki, S. *FEBS J.* **2010**, *277*, 4205.
28. Park, J.-H.; Ko, S.; Park, H. *Bull. Korean Chem. Soc.* **2008**, *29*, 921.
29. Roujeinikova, A.; Raasch, C.; Sedelnikova, S.; Liebl, W.; Rice, W. *J. Mol. Biol.* **2002**, *321*(1), 149.
30. Needleman, S. B.; Wunsch, C. D. *J. Mol. Biol.* **1970**, *48*, 443.
31. Eswar, N.; Eramian, D.; Webb, B.; Shen, M. -Y.; Sali, A. Protein Structure Modeling with MODELLER. In *Methods in Molecular Biology*, Kobe, B. G. M. H. T., Ed.; Springer, 2008; Vol. 426, pp 145–159.
32. Wang, J.; Cieplak, P.; Kollman, P. A. *J. Comput. Chem.* **2000**, *21*, 1049.
33. GoldScore performs a force field based scoring function and is made up of four components: (1) protein–ligand hydrogen bond energy (external H-bond); (2) protein–ligand van der Waals energy (external vdw); (3) ligand internal van der Waals energy (internal vdw); (4) ligand intramolecular hydrogen bond energy (internal-H-bond).